

Cancer IgG, a potential prognostic marker, promotes colorectal cancer progression

Hongpeng Jiang¹, Boxi Kang², Xinmei Huang³, Yichao Yan⁴, Shan Wang¹, Yingjiang Ye¹, Zhanlong Shen¹

¹Department of Gastroenterological Surgery, Laboratory of Surgical Oncology, Beijing Key Laboratory of Colorectal Cancer Diagnosis and Treatment Research, Peking University People's Hospital, Beijing 100044, China; ²School of Life Sciences, Peking University, Beijing 100871, China; ³Department of Immunology, School of Basic Medical Sciences, Peking University, Beijing 100191, China; ⁴Department of Gastroenterological Surgery, Peking University International Hospital, Beijing 102206, China

Correspondence to: Yingjiang Ye. Department of Gastroenterological Surgery, Laboratory of Surgical Oncology, Beijing Key Laboratory of Colorectal Cancer Diagnosis and Treatment Research, Peking University People's Hospital, Beijing 100044, China. Email: yeyingjiang@pkuph.edu.cn; Zhanlong Shen. Department of Gastroenterological Surgery, Laboratory of Surgical Oncology, Beijing Key Laboratory of Colorectal Cancer Diagnosis and Treatment Research, Peking University People's Hospital, Beijing 100044, China. Email: shenlong1977@163.com.

Abstract

Objective: Currently, no satisfactory targets for colorectal cancer or markers for immunotherapy and diagnosis and prognosis are available. Immunoglobulin G (IgG) is widely expressed in many cancers, and it promotes cancer progression. This study explored the role of cancer-derived IgG (CIgG) in colorectal cancer.

Methods: First, using a monoclonal antibody to CIgG, we examined the expression levels of CIgG in colorectal cancer cell lines by western blot and immunofluorescence analyses and in tissue specimens by immunohistochemistry. Second, the variable region gene was amplified by nested polymerase chain reaction (PCR), and PCR products were sequenced and analyzed. Third, we investigated the effect of CIgG on colorectal cancer cells by cell proliferation, wound healing, migration and invasion assays, and colony formation assay. Fourth, we performed *in vivo* tumorigenicity experiments to explore the effect of CIgG on tumorigenicity. Finally, we used RNA-seq analysis and co-immunoprecipitation experiments to further clarify possible mechanisms of CIgG.

Results: We found that CIgG is widely expressed in colorectal cancer cells, and the overexpression of CIgG indicates significantly poor colorectal cancer prognosis. Furthermore, CIgG knockdown significantly inhibits the proliferation, migration and invasion ability of cells, and tumor growth *in vivo*. RNA-seq analysis indicated that CIgG knockdown results primarily in changes in expression of apical junction and epithelial-mesenchymal transition-related genes. CIgG may be involved in colorectal cancer invasion and metastasis through interacting with E-cadherin.

Conclusions: CIgG is a potential human oncogene in colorectal cancer and that it has potential for application as a novel target in targeted therapy and a marker for prognostic evaluation.

Keywords: Cancer IgG; colorectal cancer; E-cadherin; prognosis

Submitted Feb 21, 2019. Accepted for publication May 17, 2019.

doi: 10.21147/j.issn.1000-9604.2019.03.12

View this article at: <https://doi.org/10.21147/j.issn.1000-9604.2019.03.12>

Introduction

Colorectal cancer, one of the most common types of cancer, has the third highest incidence rate and the fourth highest mortality rate worldwide (1). In recent years, the

incidence of colorectal cancer in China has been steadily rising, and its incidence is increasing in younger age groups (2,3). Although new surgical techniques and treatment strategies such as total mesenteric resection and “no-touch” isolation are continually being developed, the prognosis of

patients with colorectal cancer remains unsatisfactory. Metastasis is a major cause of colorectal cancer-related death. Therefore, new clinical treatments for colorectal cancer are urgently needed. Tumor immunotherapy has shown great promise, but immunotherapy, especially immunocytotherapy, depends on the availability of specific targets on tumors. However, at present, there is no effective specific target for immunocytotherapy or targeted therapy in colorectal cancer. In addition, although molecular markers such as carcinoembryonic antigen (CEA), carbohydrate antigen (CA)125 and CA19-9 have been widely used in clinical diagnosis and prognostic evaluation, no markers are available to provide critical information for the early diagnosis and management of colorectal cancer patients (4,5). Therefore, new molecular markers must be identified as a supplement to the current markers.

Accumulating evidence shows that immunoglobulins (Igs), especially IgG, are highly expressed in a variety of non-B cells from a variety of tumor tissues, including breast carcinoma (6), esophagus carcinoma (7), lung cancer (8,9), prostate cancer (10), bladder cancer (11), papillary thyroid cancer (12) and colorectal cancer (13). Since the discovery of Ig expression in non-B cell tissues (14,15), this topic has received increasing attention. There is strong evidence that IgG in cancerous tissues is derived from cancer cells themselves (8,11). Therefore, this non-B cell-derived IgG has been termed cancer-derived IgG (CIgG). Studies have suggested that CIgG is more likely to lead to malignant biological behavior than to exert antibody functions (8,9,11,14-18), in contrast to the traditional understanding that IgG is produced by B-lineage lymphocytes and is an important part of the immune response. Recently, the heavy chain of CIgG has been found to have a special epitope containing non-classical N-glycosylation sites on the CH1 domain, and the N-glycan structure is essential for the progression of lung squamous cancer via activation of the FAK pathway (8). Importantly, the N-glycan structure can be recognized by a monoclonal antibody (RP215) chain (8,19,20). RP215 was first discovered in 1997 by Gregory Lee *et al.* (21) in one of 3,000 hybridomas from mice immunized with cell extract from OC-3-VGH ovarian cancer cells. RP215 has been found to recognize only some cancer cells but not normal cells. However, for a long time, the nature of the antigen recognized by RP215 was unclear. In recent years, substantial evidence has indicated that RP215 specifically recognizes CIgG but not B cell-derived IgG or mesenchymal tumor-derived IgG

(8,20). However, the expression pattern of CIgG recognized by RP215 in colorectal cancer remains unidentified to date.

In this study, we first investigated the expression patterns of CIgG in colorectal cancer through immunohistochemistry analysis using RP215, and we found that RP215 recognizes primarily cancer cells but not normal colorectal epithelial cells. The high expression of CIgG indicates poor colorectal cancer prognosis. Next, we further confirmed the IgG expression in colorectal cancer cell lines, and explored the role of CIgG in colorectal cancer progression by knocking down CIgG. We found that CIgG may play an important role in the progression of colorectal cancer by interacting with E-cadherin.

Materials and methods

Cell culture and reagents

SW480, SW620, HT-29, HCT-8 and HCT-116 cell lines were obtained from the Cell Bank of the Chinese Academy of Sciences (Beijing, China). SW480 and HCT-116 cells were both maintained in IMDM (Gibco, USA) supplemented with 10% fetal bovine serum (FBS). HT-29, SW620 and HCT-8 cells were maintained in 1640 medium (Gibco, USA) supplemented with 10% FBS.

Protein extraction and western blot analysis

Total protein was extracted with RIPA lysis buffer. The protein concentration was determined through the BCA method (Kangwei Century Co., Ltd., Beijing, China). Protein samples (25 µg) were separated by 8% sodium dodecyl sulfate-polyacrylamide gel electrophoresis (SDS-PAGE) and transferred to a polyvinylidene fluoride membrane (Millipore, USA). The membrane was blocked in 5% non-fat milk for 1 h at room temperature, incubated overnight at 4 °C with primary antibodies and subsequently incubated with conjugated secondary antibody for 1 h at room temperature. Immunoreactive bands were detected with SuperSignal West Pico Chemiluminescent Substrate (Thermo Fisher Scientific, Inc., USA).

Immunofluorescence

Colorectal cancer cells were seeded in chamber slides. The cells were washed twice and fixed with 4% formaldehyde. After incubation in blocking buffer (5% BSA), primary antibodies were applied to the cells and incubated overnight. After being washed three times with PBS, the

cells were incubated with the secondary antibodies for 1 h in the dark at room temperature. After being washed three more times with PBS, the cells were coverslipped with antifade mounting medium containing 2-(4-amidinophenyl)-6-indolecarbamide dihydrochloride (DAPI).

Nested and touchdown PCR and analysis of gene rearrangement

Nested PCR was used to amplify the variable region gene in SW480 cells. In the first round of PCR, touchdown PCR was used to increase the specificity and sensitivity of the PCR amplification. The upstream primers were VH1-FR1 (5'-GAGGTGCAGCTCGAGGAGTCTGGG-3'), VH2-FR1 (5'-CAGGTGCAGCTCGAGCAGTCTGGG-3'), VH3-FR1 (5'-CAGGTACAGCTCGAGCAGT CAGG-3') and VH4-FR1 (5'-CAGGTGCAGCTGCTCGA GTCGGG-3'), and the downstream primer was a CH1 region primer (5'-ACACCGTCACCGGTTTCGG-3'). PCR was performed with a 2× Taq PCR Master Mix kit (Biomed, China). The reaction conditions of the touchdown PCR were as follows: denaturation at 94 °C for 5 min, denaturation at 94 °C for 30 s, annealing at 59 °C for 30 s, polymerization at 72 °C for 30 s for the first cycle, 17 cycles with decreases of 2 °C increments at each annealing, 20 cycles with the same annealing conditions at 47 °C for 30 s and a final elongation step for 7 min at 72 °C. In the second round of PCR, the upstream primer was VH-FR2 (5'-TGGRTCCGVCAGSCYCCNGG-3'), which was coupled with the downstream primer JH (5'-AACTGCAGAGGAGACGGTGACC-3'). The reaction conditions for the second round of PCR were as follows: pre-incubation at 95 °C for 15 min, 38 cycles of denaturation at 94 °C for 1.5 min, annealing at 57 °C for 1.5 min, polymerization at 72 °C for 3 min and a final extension step at 72 °C for 7 min.

The PCR products were cloned into a pGEM-T Easy Vector (Promega Co., Madison, WI, USA) and sequenced with an ABI3100 DNA sequencer (Thermo Fisher Scientific, Applied Biosystems, Waltham, MA, USA). The V_HD_{J_H} sequences were analyzed with the Basic Local Alignment Search Tool (BLAST).

Tissue microarray and immunohistochemistry analysis

Tissue microarrays were obtained from the tissue specimen bank of Shanghai Xinchao Biological Technology Co., Ltd. Clinicopathological features such as the TNM stage, tumor

size, histological stage, lymph node metastasis and survival were recorded. The follow-up time was 60 months. Overall survival (OS) was determined from the first surgery to the date of death or last follow-up.

Tissues were deparaffinized and rehydrated, and the antigen was retrieved by boiling in 1 mmol/L Tris/EDTA buffer (pH 9.0) in a microwave oven. After being washed with PBS, tissues were blocked with 10% normal goat serum for 30 min and incubated with primary antibodies overnight at 4 °C. Immunostaining was performed with an Envision™ ABC kit (GeneTech Co., Ltd., Shanghai, China). A pathologist independently evaluated the extent and intensity of RP215 staining and was blinded to the clinical data. Immunoreactivity in the cytoplasm was quantified as described previously (8). The percentage staining intensity was recorded, including negative staining (0), weak staining (1+), moderate staining (2+) and strong staining (3+). The staining intensity scores were then multiplied by the corresponding percentage of staining. Scores were defined as low (<100), moderate (100–200) and high (200–300).

siRNA synthesis and cell transfection

Two human siRNA sequences were designed against the constant region of the non-B Ig γ-chain: siRNA-1 (5'-GGUGGACAAGACAGUUGAG-3') and siRNA-2 (5'-AGUGCAAGGUCUCCAACAA-3'). A negative control siRNA (siNC) was synthesized by Shanghai GenePharma Co., Ltd. (Shanghai, China). The siRNAs were transfected into the SW480 cell line with Lipofectamine 3000 (Thermo Fisher Scientific) for 48 h, and then incubated in IMDM with 10% FBS for 48 h. The knockdown efficiency of IgG was verified by western blot analysis.

Cell proliferation assays

SW480 cells were plated in 96-well plates at a density of 2,000 cells/well. The cell viability was assessed on d 1, 2, 3, 4 and 5. Cell counting Kit-8 (CCK8) (10 μL, Dojindo Laboratories, Japan) was added into each well. After 4 h of incubation, the optical density of each well was measured at 450 nm with an enzyme linked immunosorbent assay (ELISA) reader (Bio-Rad).

Wound healing assay

Cells were cultured in six-well plates until about 90% of cell confluence was reached. Then, the confluent monolayer of SW480 cells was wounded with a 200-μL

sterile pipette. Images were captured at 0, 24 and 48 h to assess wound closure.

Invasion assays

SW480 cell invasion were assayed in a Transwell chamber with 8 μm pores (Corning). The lower compartment of the chamber was filled with 10% FBS. A total of 1×10^5 cells were seeded into the upper compartment. After 48 h of incubation, respectively, the membranes were fixed and stained with 0.1% crystal violet for microscopic analysis.

Colony formation assays

SW480 cells were plated in six-well plates (500 cells/well) and cultured for 14 d to allow colony formation. Then the cells were fixed and stained with 0.1% crystal violet for counting.

Transfection of SW480 cells with shRNAs and RNA-seq of transfected cells

The lentiviral vector pGLV3/H1/GFP+puro vector -siRNA-1 was produced by Shanghai GenePharma Co., Ltd. (Shanghai, China) and transfected into SW480 cells at a multiplicity of infection of 40. As a negative control (shNC), empty shRNA transfer vector was used. After six rounds of puromycin selection, RNA-Seq analysis was performed on the transfected SW480 cells.

Total RNA was extracted from the transfected SW480 cells with TRIzol reagent (Invitrogen, Carlsbad, CA, USA). cDNA library construction and Illumina sequencing of the samples were performed at Novogene Bioinformatics Technology Co., Ltd. (Beijing, China). Briefly, sequencing libraries were generated with a NEBNext® Ultra™ RNA Library Prep Kit for Illumina® (NEB, USA) according to the manufacturer's recommendations, and index codes were added to attribute sequences to each sample. The clustering of the index-coded samples was performed on a cBot Cluster Generation System with a TruSeq PE Cluster Kit v3-cBot-HS (Illumina) according to the manufacturer's instructions. After cluster generation, the library preparations were sequenced on the Illumina HiSeq platform, and 125 bp/150 bp paired-end reads were generated. After quality control and quantification of gene expression, Gene Ontology and Kyoto Encyclopedia of Genes and Genomes (KEGG) enrichment analyses of differentially expressed genes were performed with the clusterProfiler R package (Version 3.12.0; Bioconductor).

In vivo tumorigenicity experiments

Animal studies were performed in compliance with the Institutional Animal Care and Use Committee of Peking University People's Hospital. To explore the effect of CIgG on tumorigenicity, we performed subcutaneous injection of CIgG-shRNA1 and shNC stably transfected SW480 cells into BALB/c nude mice. The mice were randomized into two groups ($n=6$ per group), and approximately 1.0×10^6 cells in 100 μL of PBS were injected into 6- to 8-week-old female mice. Tumor growth after inoculation was monitored for up to 40 d, and then all mice were sacrificed. Tumor diameters were measured with a caliper, and tumor volume was calculated as $(\text{width}^2 \times \text{length})/2$.

Statistical analysis

Data are presented as $\bar{x} \pm s$. Statistical analyses were performed with *t*-test for two groups or one-way analysis of variance (ANOVA) followed by *t*-test for three or more groups. Multivariate survival analysis was carried out by using Cox's regression model. Kaplan-Meier analyses were performed for analysis of survival times according to the RP215-CIgG expression levels. All tests were two-sided, and $P < 0.05$ was considered statistically significant. Data analysis was performed using IBM SPSS Statistics (Version 20.0; IBM Corp., New York, USA) and GraphPad Prism 7.0 software (GraphPad, San Diego, USA).

Results

CIgG significantly indicated poor colorectal cancer prognosis

Tissue microarrays comprised samples from 100 patients with colorectal cancer, including 80 matched tumor and normal tissue samples, and 20 tumor tissue samples. Using immunohistochemistry, we first investigated the differences in immunostaining patterns between the RP215 and commercial anti-IgG antibody in colorectal cancer and normal tissues. The results revealed that CIgG was mainly distributed within the cancer nest of cancer tissues, whereas commercial anti-IgG recognized both cancer cells and stromal cells of colorectal tissues (*Figure 1A*). Subsequently, we used a tissue microarray of cancer tissues and RP215 immunohistochemistry to analyze the correlation between CIgG expression and clinical and pathological characteristics. We found that CH1-related glycosylated CIgG was mainly distributed in the cancer nest of cancer

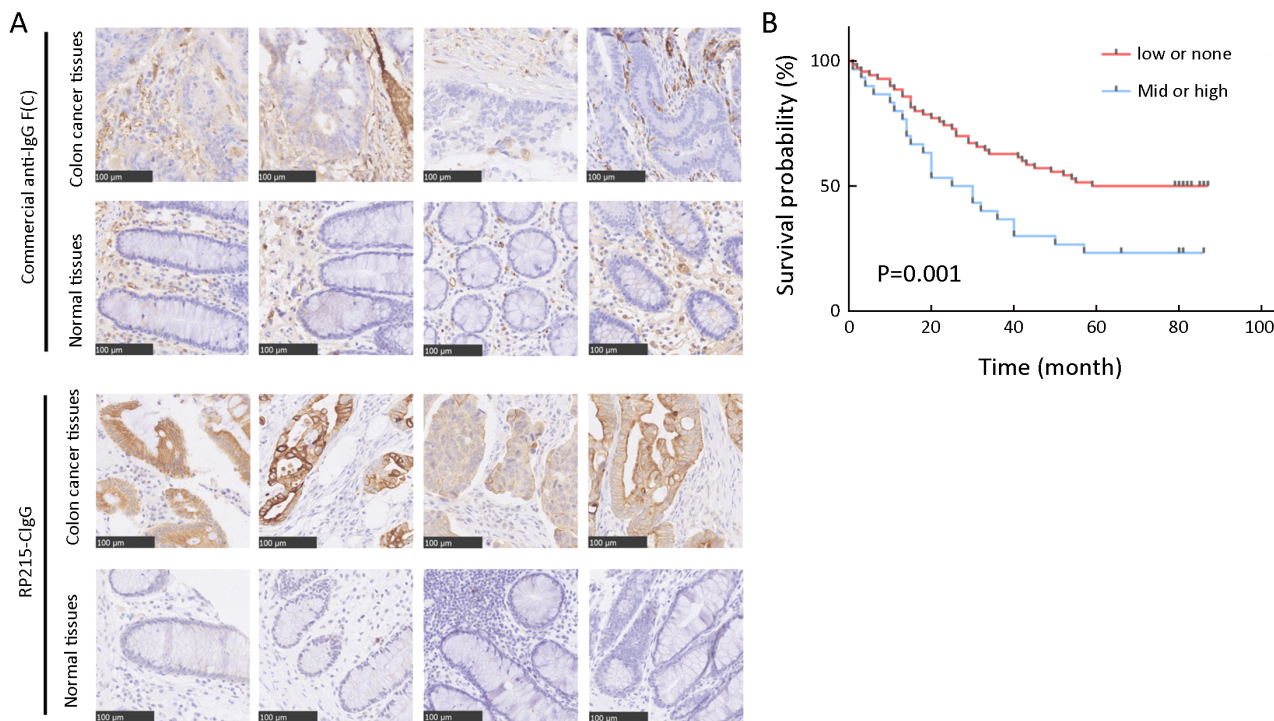


Figure 1 Cancer-derived IgG (CIgG) expression in colorectal cancer and normal tissues. (A) Immunohistochemistry (IHC) analysis of CIgG expression in colorectal cancer and normal tissues. Scale bars, 100 μm; (B) Kaplan-Meier survival analysis showed that moderate/high CIgG expression (staining score >100) in colorectal cancer tissue predicted worse overall survival (OS) compared with low or no CIgG expression (staining score ≤100) (P=0.001).

tissues (55/100, 55%) compared with that in normal tissues adjacent to cancer tissues (6/80, 7.5%). Moreover, all positive CIgG staining in normal tissues showed low intensity. Additionally, the proportions of moderate/high expression of CIgG in cancer tissues were significantly higher (30/100, 30%) than those with low expression of CIgG (25/100, 25%). Kaplan-Meier survival analysis showed that moderate/high CIgG expression in colorectal cancer tissue predicted worse OS compared with low or no CIgG expression (P=0.001) (Figure 1B). Then, multivariate Cox regression analysis demonstrated that CIgG staining intensity, lymph node metastasis, TNM stage, and tumor location were independent prognostic factors with regard to 5-year OS (Table 1).

CIgG is frequently expressed in colorectal cancer cell lines

To address whether the expression of CH1-related glycosylated CIgG might be observed in colorectal cell lines, we detected the CIgG in five colorectal cell lines, HT-29, HCT-116, HCT-8, SW620 and SW480, by western blot. The results showed expression of RP215-

recognized CIgG in HT-29, HCT-8 and SW480, but not in HCT-116 and SW620. However, the IgG heavy chain was found in HCT-116, and the Ig light chain (κ chain) was found in all colorectal cancer cell lines by using commercial anti-IgG heavy chain or anti-human Igκ chain antibodies, respectively. The SW480 cell line showed the highest CIgG expression among all examined cell lines (Figure 2A). Immunofluorescence analysis also indicated higher CIgG expression in SW480 than in HCT-116 cells; and the CIgG was mainly localized in the cytosol, cytomembrane and extracellular matrix of the cancer cells (Figure 2B).

To further verify that CIgG is produced by colorectal cancer cells, rearranged transcripts of the IgG heavy chain in SW480 cells were amplified and analyzed. As expected, the functional VDJ rearrangement of CIgG heavy chain was found in the colorectal cancer cell line. Moreover, similarly to previous findings (11,22-24), the VDJ recombination of IgH variable region (V_HDJ_H) of SW480-derived IgG showed restrictive diversity, and IGHV3-23/IGHD3-22/IGHJ4 appeared at a high frequency (Figure 2C).

Knockdown of CIgG inhibited SW480 cell proliferation, migration and invasion in vitro, and tumor growth in vivo

To determine the role of CIgG in colorectal cancer progression, we knocked down CIgG in SW480 to elucidate the role of CIgG in tumor progression. Using siRNA or siNC in SW480 cells, we down-regulated the CIgG expression (Figure 3A). Because of the sequence complexity of the immunoglobulin variable region, we used two siRNAs targeting the constant region. CIgG knockdown significantly inhibited cell growth in CCK8 cell proliferation assays (Figure 3B) and decreased colony formation ability (siRNA-1 vs. siNC, $P=0.014$; siRNA-2 vs. siNC, $P=0.001$) (Figure 3D). Subsequently, we assessed cell migration by using wound healing assays. The knockdown of CIgG suppressed the wound healing ability of SW480 cells (24 h wound healing: siRNA-1 vs. siNC, $P=0.014$; siRNA-2 vs. siNC, $P=0.002$; 48 h wound healing: siRNA-1 vs. siNC, $P=0.002$; siRNA-2 vs. siNC, $P=0.002$) (Figure 3C). Similarly, the siRNAs significantly decreased the invasion of SW480 cells (siRNA-1 vs. siNC, $P=0.007$; siRNA-2 vs. siNC, $P=0.006$) (Figure 3E).

In addition, we determined whether knockdown of CIgG might inhibit tumor growth *in vivo*. SW480 cells with or without CIgG knockdown were injected subcutaneously into nude mice to establish a colorectal cancer-bearing

model, and tumor growth rates observed. We found that the tumor growth rate was significantly inhibited in the shRNA group ($n=6$) compared with the control group ($n=6$) (Figure 3F). The average tumor size and weight in the shRNA group were significantly lower than those in the control group ($P=0.028$, $P=0.029$, respectively; Figure 3F).

shRNA against CIgG primarily results in changes in expression of apical junction and epithelial-mesenchymal transition-related genes

To further investigate the mechanism underlying CIgG's role in cancer cells, we performed CIgG RNA interference with shRNAs in SW480 cells. RNA-seq was then performed to profile the transcriptomic changes. In the shRNA-1 transfected group compared with the shNC group, a total of 268 differentially expressed genes (DEGs) were identified, including 71 down-regulated and 197 up-regulated genes (Figure 4A). Among the cellular component (CC) gene ontologies, DEGs showed enrichment in terms related to the plasma membrane, the transmembrane complex and extracellular matrix, whereas the top-enriched biological process ontologies were related to developmental processes and cell differentiation. In addition, the top-enriched molecular function terms were receptor-ligand binding and transporter activity (Figure 4C). Specifically, DEGs in the top-enriched CC terms, which were related to

Table 1 Cox's proportional hazards model analysis of prognostic factors in patients with colorectal cancer

Variables	HR	95% CI	P
CIgG staining (None-low vs. Mid-high)	0.467	0.248–0.879	0.018
Gender (Male vs. Female)	1.242	0.682–2.261	0.478
Age (<60 vs. ≥60 years)	1.819	0.881–3.754	0.106
Tumor size (≥5 vs. <5 cm)	0.531	0.278–1.015	0.056
Tumor location			
Ascending	–	–	0.299
Hepatic flexure	1.391	0.632–3.059	0.412
Transverse	1.846	0.781–4.363	0.162
Splenic flexure	4.373	1.055–18.123	0.042
Descending	0.431	0.052–3.571	0.436
Sigmoid	1.182	0.417–3.345	0.753
Histological grade (I–II vs. III–IV)	1.513	0.806–2.843	0.198
Infiltration depth (T1–T2 vs. T3–T4)	1.080	0.122–9.583	0.945
Lymph node metastasis (N0 vs. N1–N2)	0.391	0.204–0.748	0.005
Metastasis (M0 vs. M1)	0.445	0.170–1.165	0.099
TNM stage (I–II vs. III–IV)	0.498	0.277–0.895	0.020

CIgG, cancer-derived IgG; HR, hazard ratio; 95% CI, 95% confidence interval.

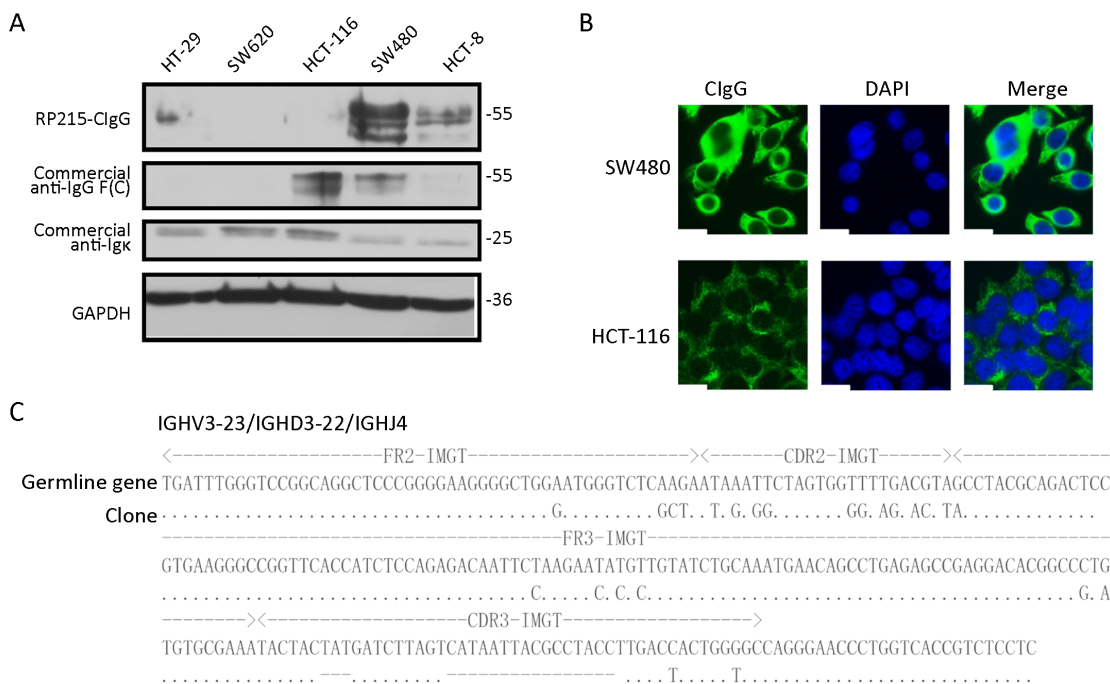


Figure 2 Cancer-derived IgG (CIgG) expression in colorectal cancer cells and transcripts with a unique pattern of V_HDJ_H rearrangement. (A) Lysates of colorectal cancer cells, including HT-29, SW620, HCT-116, SW480 and HCT-8, were analyzed by western blot using RP215 or commercial anti-human IgG antibody [anti-IgG F(C) and anti-Ig κ]; (B) Localization of RP215-CIgG in SW480 and HCT-116 cells was analyzed by immunofluorescence staining using RP215 (green). Scale bars, 50 μ m; (C) SW480 cells' sequences carrying V_HDJ_H compared with the best matching functional germline gene. Dots, identical sequences; capital letters, mutant parts.

components of the plasma membrane, showed substantial up-regulation in the shRNA-1 group (Figure 4C). We next performed enrichment analysis on the hallmark gene sets from MSigDB and the reference pathways in the KEGG database. Apical junction and epithelial-mesenchymal transition terms were among the significantly enriched MSigDB gene sets, and the top-enriched KEGG pathways included cell adhesion, extracellular matrix receptor interaction and focal adhesion (Figure 4B).

To better understand the mechanism underlying the preference of colorectal cancer cells to interact with components of the plasma membrane, as indicated by the RNA-Seq results, we analyzed the protein complexes generated by co-immunoprecipitation (Co-IP) with RP215. We focused on the plasma membrane proteins E-cadherin and β -catenin, among the proteins identified by liquid chromatography-tandem-mass spectrometry analysis. Western blot analysis revealed that RP215 pulled down both E-cadherin and β -catenin (Figure 4D). After CIgG knockdown, the expression of E-cadherin increased, and the expression of c-Myc decreased (Figure 4E). Immunofluorescence analysis demonstrated that the knockdown of

CIgG attenuated the fluorescence intensity at adherens junctions between cells (Figure 4F).

Discussion

The roles of non-B cell IgG are rapidly being revealed, largely through use of the CIgG-specific antibody RP215. Although RP215 and non-B cell IgG were discovered by different research teams 20 years ago, the researchers did not initially link the two (21,25). Lee *et al.* (19,20,26) thought that RP215 mainly recognizes a cancer-associated antigen, CA215, which has been detected as a pan cancer marker in many types of human cancerous tissues. It was not until recently that the antigen recognized by RP215 was discovered to be CIgG, which is expressed by many cancer cells (26,27). Before that point, studies on CIgG mainly depended on commercial IgG antibodies; therefore, previous research on immunohistochemistry reactions using commercial IgG antibodies may not be sufficient to demonstrate that all positive reactions are caused by CIgG (5,10,12,13,28). In this report, we showed that when the expression of CIgG is inhibited by shRNA in SW480 cells, growth, migration and invasion are suppressed *in vitro*.

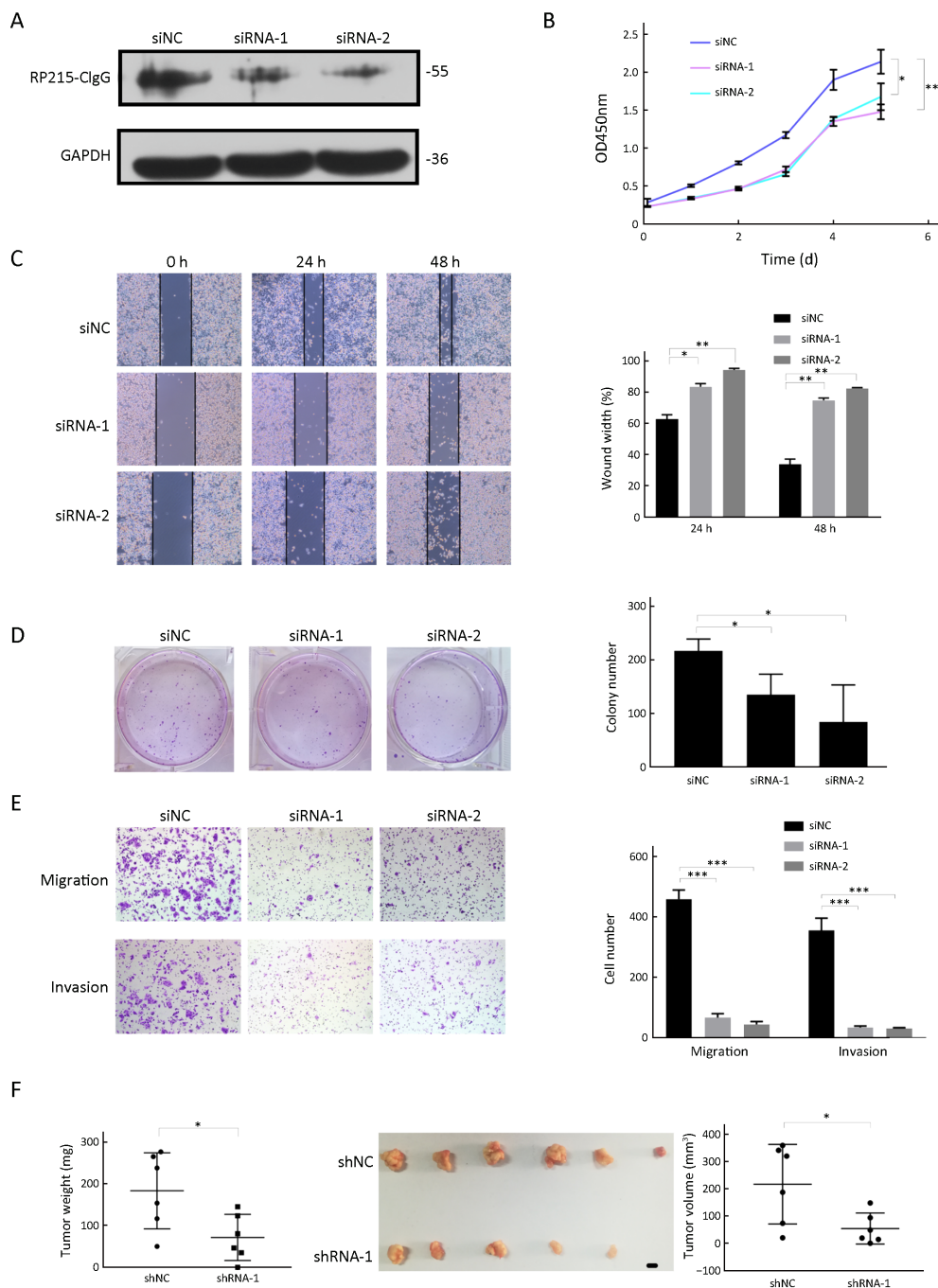


Figure 3 Knockdown of cancer-derived IgG (CIgG) inhibited SW480 cell proliferation, invasion and migration. (A) Western blot showed that CIgG was down-regulated in colorectal cancer cells after transfection with siRNAs; (B) Knockdown of non-B-IgG inhibited proliferation of SW480 cells. The relative growth (OD values) was assessed with cell counting Kit-8 assays. *, $P < 0.05$; **, $P < 0.01$. siNC, normal control siRNA; siRNA, small interfering RNA; OD, optical density; (C) Wound healing assay was performed on SW480 cells treated with siRNAs or siNC. The wound breadth was measured at the indicated time points; (D) SW480 cells were treated with siRNAs or siNC for 48 h. The plates were stained and photographed 14 d later. Colony percentages were calculated; (E) CIgG inhibition suppresses SW480 cell migration and invasion; (F) Suppression of tumor growth by inhibition of CIgG in SW480 cell subcutaneous xenografts. Scale bar, 5 mm.

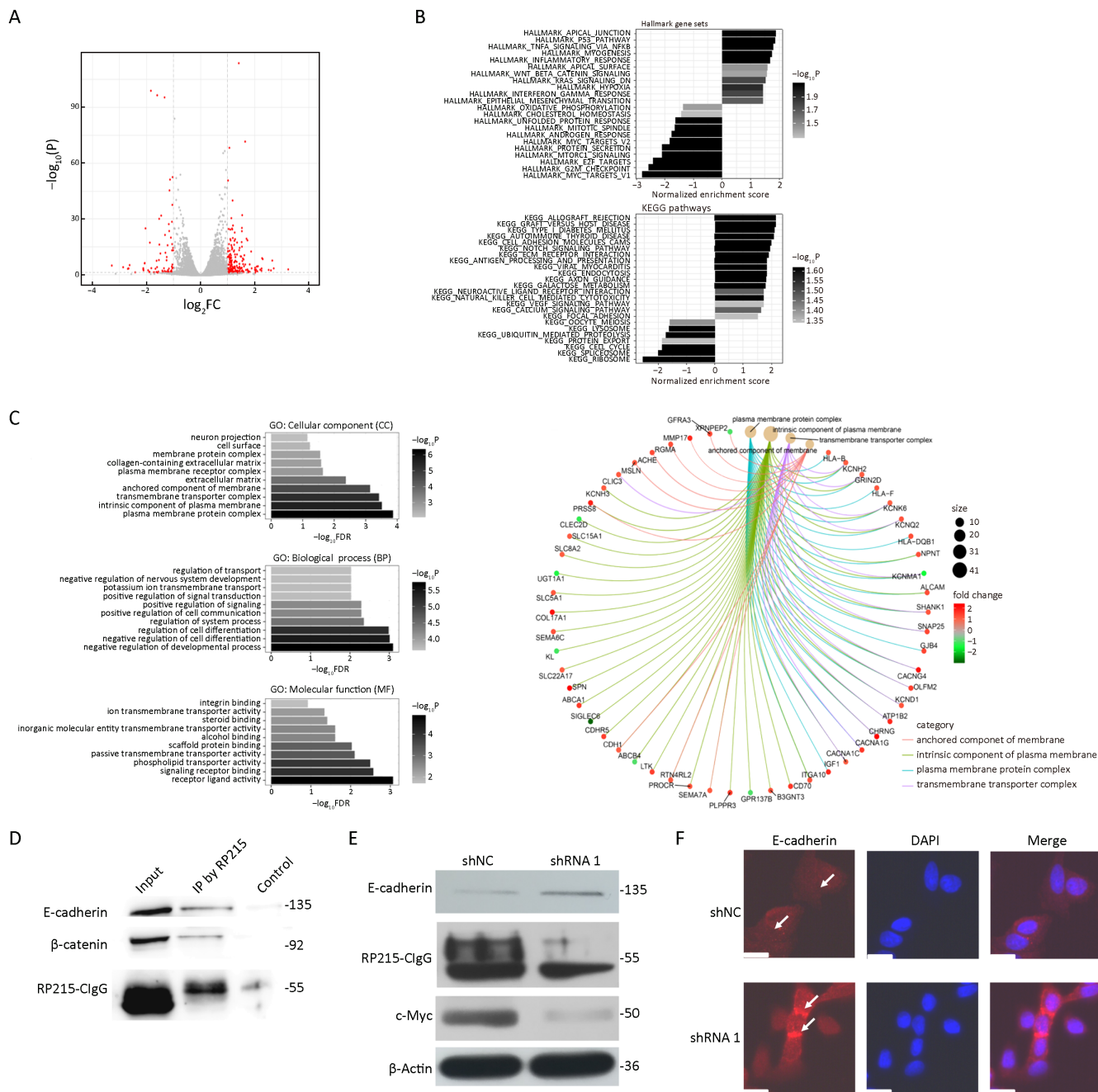


Figure 4 Cancer-derived IgG (CIgG) may play a key role by interacting with membrane E-cadherin. (A) Up-regulated and down-regulated differentially expressed genes (DEGs) in shRNA-1 vs. shNC transfected SW480 cells; (B) Kyoto Encyclopedia of Genes and Genomes (KEGG) pathways and hallmark gene set annotations of DEGs; (C) Gene Ontology categorization of DEGs; (D) Total cell lysates from SW480 cells were extracted and subjected to immunoprecipitation assays using RP215. Western blots were performed for E-cadherin, β -catenin or RP215-CIgG; (E) Total cell lysates from SW480 cells, transfected with shRNA-1 or shNC, were analyzed by western blot with antibodies to E-cadherin, c-Myc or β -Actin; (F) E-cadherin was analyzed by immunofluorescence (IF) staining. Arrows, adherens junctions. Scale bars, 50 μ m.

Analysis of CIgG expression with RP215 in a group of colorectal cancer and normal tissues suggested that CIgG is expressed primarily within the cancer nest of cancer tissues, and a strong positive correlation was observed between the expression of CIgG and poor prognosis of patients with colorectal cancer.

On the basis of our data, the IgG expression determined with a commercial IgG antibody differed between colorectal cancer and normal tissues, whereas a large proportion of positive expression was found in the stroma of cancer tissues. This finding suggested that the positive staining reaction of general IgG antibody may be partly derived from infiltrating lymphocytes in the cancer tissues, which is clearly different from those for CIgG. In contrast, positive staining of CIgG was observed mainly in the cancer nest of cancer tissues; hence RP215 can be used to distinguish between cancerous tissues and normal tissues. Moreover, CIgG showed promising value in predicting patient prognosis: its statistical strength was even stronger than that of TNM staging, an evaluation index used for prognosis in clinical applications. CIgG staining intensity, lymph node metastasis, TNM stage, and tumor location may have value in the prognosis of patients with colorectal cancer in the present cohort. Researchers should consider the potential value of using CIgG to distinguish cancer from adjacent tissues and predict the prognosis of patients.

The non-B cell-derived Ig heavy chain displays a restricted diversity, which is different from the diversity of B cell-derived Ig. Similarly, V_HDJ_H rearrangements of colorectal cancer cell-derived CIgG transcripts also showed unique patterns. Sheng *et al.* (11) have reported that *IGHV3-30* is the most used gene in bladder cancer cells. Zheng *et al.* (29) have used the laser capture microdissection method to capture breast cancer cells and have found new V_HDJ_H recombination sequences without homology to known sequences for tumor-infiltrating B-lymphocytes. A recently published study by Geng *et al.* (24) has reported that the sequence of variable regions in colorectal cancer has a limited rearrangement pattern. In this study, we found that *IGHV3-23* was a frequently encountered sequence in 4 clones from SW480 cells. The potential mechanism for colorectal cancer progression of these unique and predominantly frequent sequences in epithelial tumor cells requires further study.

The role of CIgG in the development of cancer has been most studied in lung cancer (8,9,17), followed by urinary tumors (11,16). Recently, new progress in lung cancer studies has been reported. Tang *et al.* (8) have demonstrated that CIgG interacts with integrin $\alpha6\beta4$ and

consequently activates FAK/Src pathways by promoting phosphorylation of FAK and SRC. In the present study, through omics, we sought to identify CIgG-related signaling pathways in colorectal cancer. Enrichment analysis revealed that CIgG may be related to components of the plasma membrane. This mechanism through which CIgG regulates the development of colorectal cancer should be explored in detail in future research. Most E-cadherin, under normal circumstances, is present in an E-cadherin/catenin complex located in adherens junctions at the cell membrane, and it provides important strength in cell-cell adhesion (30,31). Our Co-IP analysis revealed that RP215-CIgG directly interacts with E-cadherin and β -catenin. After inhibition of the expression of CIgG, the expression of E-cadherin at the adherens junctions increased, and that of c-Myc was significantly attenuated. Oncogenes, such as *TET2* and *ICAT*, can activate the Wnt/ β -catenin signaling pathway by disrupting the E-cadherin/ β -catenin complex and promoting β -catenin nuclear translocation (32,33). As a well-established Wnt target gene, c-Myc was one of the direct targets transcribed by β -catenin (34,35). We therefore speculate that CIgG may cause E-cadherin to dissociate from adherens junctions and activate β -catenin/c-Myc signaling by regulating β -catenin nuclear translocation, thereby promoting cancer invasion and metastasis. Additional research is needed to clarify the relevance of these findings.

Conclusions

Our study showed that colorectal cancer cells themselves express CIgG and that *IGHV3-23* is present in CIgG transcripts of SW480 cells. In addition, CIgG may be involved in colorectal cancer invasion and metastasis through interacting with E-cadherin. More importantly, CIgG may be a promising maker for predicting the prognosis of patients with colorectal cancer.

Acknowledgements

This present study was supported by grants from the National Natural Science Foundation of China (No. 8157101395) and Beijing Natural Science Foundation (No. 7182171).

Footnote

Conflicts of Interest: The authors have no conflicts of interest to declare.

References

1. Torre LA, Bray F, Siegel RL, et al. Global cancer statistics, 2012. *CA Cancer J Clin* 2015;65:87-108.
2. Chen W, Zheng R, Zhang S, et al. Cancer incidence and mortality in China in 2013: an analysis based on urbanization level. *Chin J Cancer Res* 2017;29:1-10.
3. Chen W, Sun K, Zheng R, et al. Cancer incidence and mortality in China, 2014. *Chin J Cancer Res* 2018;30:1-12.
4. Zhong W, Yu Z, Zhan J, et al. Association of serum levels of CEA, CA199, CA125, CYFRA21-1 and CA72-4 and disease characteristics in colorectal cancer. *Pathol Oncol Res* 2015;21:83-95.
5. Zhao J, Gu J, Yang Z, et al. Relationship among CEA expression in tumor, CEA serum level and radio-immunoguided surgery in colorectal cancer. *Chin J Cancer Res* 2003;15:269-72.
6. Yang B, Ma C, Chen Z, et al. Correlation of immunoglobulin G expression and histological subtype and stage in breast cancer. *PLoS One* 2013;8:e58706.
7. Zhang L, Hu S, Korteweg C, et al. Expression of immunoglobulin G in esophageal squamous cell carcinomas and its association with tumor grade and Ki67. *Hum Pathol* 2012;43:423-34.
8. Tang J, Zhang J, Liu Y, et al. Lung squamous cell carcinoma cells express non-canonically glycosylated IgG that activates integrin-FAK signaling. *Cancer Lett* 2018;430:148-59.
9. Jiang C, Huang T, Wang Y, et al. Immunoglobulin G expression in lung cancer and its effects on metastasis. *PLoS One* 2014;9:e97359.
10. Liu Y, Chen Z, Niu N, et al. IgG gene expression and its possible significance in prostate cancers. *Prostate* 2012;72:690-701.
11. Sheng Z, Liu Y, Qin C, et al. Involvement of cancer-derived IgG in the proliferation, migration and invasion of bladder cancer cells. *Oncol Lett* 2016;12:5113-21.
12. Qiu Y, Korteweg C, Chen Z, et al. Immunoglobulin G expression and its colocalization with complement proteins in papillary thyroid cancer. *Mod Pathol* 2012;25:36-45.
13. Niu N, Zhang J, Huang T, et al. IgG expression in human colorectal cancer and its relationship to cancer cell behaviors. *PLoS One* 2012;7:e47362.
14. Xu Y, Chen B, Zheng S, et al. IgG silencing induces apoptosis and suppresses proliferation, migration and invasion in LNCaP prostate cancer cells. *Cell Mol Biol Lett* 2016;21:27.
15. Wang J, Lin D, Peng H, et al. Cancer-derived immunoglobulin G promotes LPS-induced pro-inflammatory cytokine production via binding to TLR4 in cervical cancer cells. *Oncotarget* 2014;5:9727-43.
16. Sheng Z, Liu Y, Qin C, et al. IgG is involved in the migration and invasion of clear cell renal cell carcinoma. *J Clin Pathol* 2016;69:497-504.
17. Liu Y, Liu D, Wang C, et al. Binding of the monoclonal antibody RP215 to immunoglobulin G in metastatic lung adenocarcinomas is correlated with poor prognosis. *Histopathology* 2015;67:645-53.
18. Li L, Cheng X, Zheng Z, et al. Overexpression of cancer cell-derived immunoglobulin G correlates with poor prognosis in gastric cancer patients. *Transl Cancer Res* 2016;5:285-93.
19. Lee G, Zhu M, Ge B, et al. Carbohydrate-associated immunodominant epitope(s) of CA215. *Immunol Invest* 2012;41:317-36.
20. Lee G, Laflamme E, Chien CH, et al. Molecular identity of a pan cancer marker, CA215. *Cancer Biol Ther* 2008;7:2007-14.
21. Lee CY, Chen KW, Sheu FS, et al. Studies of a tumor-associated antigen, COX-1, recognized by a monoclonal antibody. *Cancer Immunol Immunother* 1992;35:19-26.
22. Qiu X, Sun X, He Z, et al. Immunoglobulin gamma heavy chain gene with somatic hypermutation is frequently expressed in acute myeloid leukemia. *Leukemia* 2013;27:92-9.
23. Jiang D, Ge J, Liao Q, et al. IgG and IgA with potential microbial-binding activity are expressed by normal human skin epidermal cells. *Int J Mol Sci* 2015;16:2574-90.
24. Geng ZH, Ye CX, Huang Y, et al. Human colorectal cancer cells frequently express IgG and display unique Ig repertoire. *World J Gastrointest Oncol* 2019;11:195-207.
25. Qiu X, Yang G. Existence of Ig-like protein in malignant tumor cells. *Bai Qiu En Yi Ke Da Xue Xue Bao (in Chinese)* 1996;22:572-5.

26. Lee G, Wu Q, Li CH, et al. Recent studies of a new carbohydrate-associated pan cancer marker, CA215. *J Clin Ligand Assay* 2006;29:47-51.
27. Lee G, Zhu M, Ge B, et al. Widespread expressions of immunoglobulin superfamily proteins in cancer cells. *Cancer Immunol Immunother* 2012;61:89-99.
28. Qiu X, Zhu X, Zhang L, et al. Human epithelial cancers secrete immunoglobulin G with unidentified specificity to promote growth and survival of tumor cells. *Cancer Res* 2003;63:6488-95.
29. Zheng J, Huang J, Mao Y, et al. Immunoglobulin gene transcripts have distinct VHDJH recombination characteristics in human epithelial cancer cells. *J Biol Chem* 2009;284:13610-9.
30. Ohashi W, Yamamine N, Imura J, et al. SKL2001 suppresses colon cancer spheroid growth through regulation of the E-cadherin/ β -Catenin complex. *Biochem Biophys Res Commun* 2017;493:1342-48.
31. Bryant DM, Stow JL. The ins and outs of E-cadherin trafficking. *Trends Cell Biol* 2004;14:427-34.
32. Yang G, Zeng X, Wang M, et al. The TET2/E-cadherin/ β -catenin regulatory loop confers growth and invasion in hepatocellular carcinoma cells. *Exp Cell Res* 2018;363:218-26.
33. Jiang Y, Ren W, Wang W, et al. Inhibitor of β -catenin and TCF (ICAT) promotes cervical cancer growth and metastasis by disrupting E-cadherin/ β -catenin complex. *Oncol Rep* 2017;38:2597-606.
34. van de Wetering M, Sancho E, Verweij C, et al. The β -catenin/TCF-4 complex imposes a crypt progenitor phenotype on colorectal cancer cells. *Cell* 2002;111:241-50.
35. Li J, Yu B, Deng P, et al. KDM3 epigenetically controls tumorigenic potentials of human colorectal cancer stem cells through Wnt/ β -catenin signalling. *Nat Commun* 2017;8:15146.

Cite this article as: Jiang H, Kang B, Huang X, Yan Y, Wang S, Ye Y, Shen Z. Cancer IgG, a potential prognostic marker, promotes colorectal cancer progression. *Chin J Cancer Res* 2019;31(3):499-510. doi: 10.21147/j.issn.1000-9604.2019.03.12